Optimizing the Timing of Male Fetal NIPT Testing: A Model Based on Linear Regression, Survival Analysis, and Monte Carlo Simulation

Xinyu Wang [1, *, #], Ruoxi Zhou [1, #], Honghua Zhan [2], Lingjie Liu [1], Lu Li [1]

[1] School of Computer Science, Qufu Normal University, Rizhao, China, 276826

[2] School of Management, Qufu Normal University, Rizhao, China, 276826

* Corresponding Author Email: xinyu_wang0513@163.com

[#]These authors contributed equally.

Abstract. The accuracy of non-invasive prenatal testing (NIPT) is significantly influenced by gestational age and maternal body mass index (BMI), and individual variability makes a single standardized testing time suboptimal for both sensitivity and specificity. In this study, a univariate linear regression model was developed based on fetal Y-chromosome concentration data to examine its association with gestational age and BMI, revealing significant positive correlations for both factors ($p < 0.01$). Subsequently, K-means clustering combined with survival analysis was employed to stratify pregnant individuals into three BMI groups. Optimal testing times were estimated at 13.71, 15.14, and 19.57 weeks, respectively, using Kaplan-Meier curves, with the Log-rank test confirming significant intergroup differences. Accounting for assay variability, Monte Carlo simulation suggested a delay of 0.5–1 week in testing. Furthermore, incorporating maternal age and parity into a multivariate integrated model revealed that individuals with low BMI and prior delivery history could be tested earlier, whereas those with high BMI and no prior delivery required later testing. After optimization, recommended gestational ages were adjusted later by 0.12–0.15 weeks. Notably, in parous individuals with BMI ranging from 27.7 to 33.8, the testing time increased from 13.86 to 15.26 weeks, achieving a success rate of 84.48%.

Keywords: Non-invasive prenatal testing, Y-chromosome concentration, K-means clustering, Monte Carlo simulation.

1. Introduction

Non-invasive prenatal testing (NIPT) has become a critical clinical tool for screening fetal chromosomal abnormalities since its introduction in the early 2000s. This technique leverages cell-free fetal DNA (cffDNA) circulating in maternal peripheral blood, combined with high-throughput sequencing and bioinformatics analysis, to determine fetal chromosomal ploidy. Its clinical utility stems from both maternal safety advantages and high diagnostic accuracy, which fundamentally depends on cffDNA concentration in maternal circulation. Over the past two decades, NIPT has evolved from single-chromosome screening to multi-chromosomal analysis, achieving over 70% adoption rates in some developed countries. In China, tertiary hospitals in major cities now routinely offer NIPT as a second-trimester screening option for pregnant women. However, emerging clinical evidence reveals inherent limitations in current NIPT protocols, particularly regarding inconsistent diagnostic reliability caused by variable timing decisions and individual biological differences [1]. Premature testing often yields false-negative results or technical failures due to insufficient cffDNA levels, while delayed testing shortens the clinical intervention window for abnormal fetuses, increasing maternal psychological and physiological burdens. Maternal characteristics significantly influence cffDNA concentrations - for instance, elevated body mass index (BMI) dilutes cffDNA through expanded maternal blood volume [2], while varying maternal age-related aneuploidy risks necessitate different diagnostic thresholds [3]. These complexities challenge the universal applicability of standardized testing protocols, highlighting urgent needs for personalized NIPT frameworks tailored to individual patient profiles.

Current research efforts have systematically investigated factors affecting NIPT performance and optimal timing strategies. Li et al. [4] identified gestational age <12 weeks and BMI >30 kg/m² as key risk factors for low cffDNA concentrations through retrospective analysis, though their work remained at basic univariate correlation levels without developing quantitative timing models. Chen et al. [5] conducted systematic reviews confirming maternal BMI as a negative predictor for cffDNA levels, recommending routine testing after 12 weeks gestation - valuable insights that lacked stratified personalized timing frameworks. Gazdarica et al. [6] applied survival analysis using Kaplan-Meier estimation to demonstrate delayed cffDNA concentration milestones in high-BMI pregnancies, providing data support for BMI-stratified protocols but neglecting error margin considerations. Duboc et al. [7] developed the NiPTUNE bioinformatics pipeline to enhance accuracy through cffDNA quantification, though their model lacked integration of maternal stratification factors. Benn et al. [8] reviewed literature to identify gestational age and BMI as key cfDNA determinants. However, lacking primary data modeling and multivariate stratification, it cannot support precise individualized recommendations. Srinivasan et al. [9] used longitudinal data to reveal cfDNA dynamics and individual variability, highlighting the need for serial monitoring. However, they did not develop a generalized model for individualized timing recommendations. Van Beek et al. [10] compared quality control protocols for different cffDNA quantification methods (Y-chromosome vs genomic discontinuity approaches), revealing methodological impacts on result stability without proposing stratified control strategies.

Building upon these foundational studies, this research develops multidimensional optimization models to address critical gaps in NIPT timing precision and individual variability management. Our methodological contributions focus on three key advancements: First, quantifying the relationships between fetal Y-chromosome concentrations (for male pregnancies) and maternal gestational age/BMI to elucidate underlying biological mechanisms. Second, optimizing testing windows for male pregnancies based on BMI stratification while accounting for measurement error impacts. Third, developing enhanced stratification frameworks incorporating maternal age and obstetric history to achieve higher-resolution personalized testing protocols.

2. Study on the Correlation between Fetal Y Chromosome Concentration and Maternal Gestational Age & BMI

2.1. Methodology for Analyzing the Correlation between Fetal Y Chromosome Concentration and Maternal Gestational Age & BMI

2.1.1. Data Preprocessing

The data utilized in this study were sourced from: https: // www.mcm.edu.cn/html_cn/node/ 03c91a444e62eee81a3740fa97a461a6.html.

Removal of Invalid Data: Samples with a gestational age of less than 10 weeks or more than 25 weeks were excluded based on the applicable range for NIPT testing. Samples from non-healthy fetuses were also removed. This ensures the analysis data falls within a reasonable range and focuses on modeling healthy fetuses.

Numerical Conversion of Gestational Age and ID: Gestational age data in the "weeks + days" format was converted into floating-point values using Formula (1) to enhance continuity and facilitate modeling. Categorical variables, such as patient ID (e.g., converting "A001" to the integer 1), were also numerically mapped to avoid interference from non-numeric symbols.

$$Gestational\_Age = Weeks + \frac{Days}{7} \tag{1}$$

Here, Gestational_Age refers to the total duration of pregnancy, expressed in weeks with decimals; Weeks indicate the number of complete weeks of pregnancy; Days represent the remaining number of days beyond the complete weeks.

Handling of Missing Data: Samples containing missing values were uniformly deleted to prevent potential bias introduced by imputation, thereby ensuring data integrity.

Min-Max Normalization of Variables: Min-max normalization was applied to variables with large individual differences, such as maternal BMI and fetal Y chromosome concentration, to eliminate scale differences and enhance comparability. Gestational age was not normalized due to its naturally limited range of variation. To validate the normalization effect, z-score distribution histograms and box plots for the normalized BMI and Y chromosome concentration are shown in Figure 1.

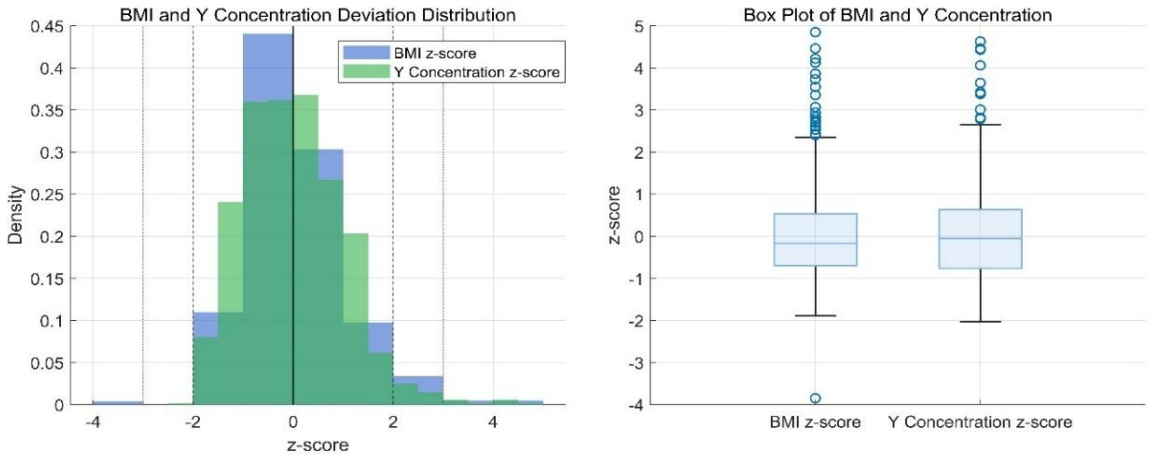

Figure 1. Distribution Histograms and Box Plots of Normalized BMI and Y Chromosome Concentration.

The distribution histograms show that both variables approximately follow a normal distribution with a mean of 0 and a standard deviation of 1. This indicates that the normalization process effectively eliminated the scale differences in the original data, placing the variables on a comparable scale. The box plots further reveal that the z-scores for the vast majority of samples are concentrated within the [-2,2] interval, exhibiting a relatively symmetrical distribution without severely deviating extreme outliers. This demonstrates that the normalized data possesses good centrality and stability, providing a necessary distribution foundation for subsequent linear regression modeling and accurate estimation of variable relationships.

Handling of Repeated Measurement Data: For records with identical gestational age and BMI from repeated tests, only the one with the highest quality was retained. This ensures sample independence and prevents estimation bias.

2.1.2. Construction of Linear Regression Models

To investigate the quantitative relationship between fetal Y chromosome concentration and gestational age/BMI, two separate simple linear regression models were constructed. The parameters of the models were estimated using the least squares method, aiming to minimize the sum of squared residuals between the predicted and actual observed values.

A regression model was established to analyze the relationship between gestational age and Y chromosome concentration:

$$y_i = \beta_1 g_i + \varepsilon_i \tag{2}$$

Here, $y_i = Y_i - \bar{Y}$ represents the mean-centered Y chromosome concentration value for the i-th sample, $g_i = G_i - \bar{G}$ represents the mean-centered gestational age value for the i-th sample, β_1 is the regression coefficient, and ε_i is the error term.

To assess the influence of BMI on Y chromosome concentration, the following model was constructed:

$$y_i = \gamma_1 b_i + \varepsilon_i \tag{3}$$

Here, $b_i = B_i - \bar{B}$ represents the mean-centered BMI value for the i-th sample, γ_1 is the regression coefficient, and ε_i is the error term.

2.1.3. Estimation of Regression Models Using the Least Squares Method

Based on the constructed linear regression models, the regression coefficients were estimated via the least squares method. This approach determines the line of best fit by minimizing the sum of squared residuals. The specific estimation formulas are as follows:

$$\hat{\beta}_1 = \frac{\sum_{i=1}^{n} g_i y_i}{\sum_{i=1}^{n} g_i^2}, \quad \hat{\gamma}_1 = \frac{\sum_{i=1}^{n} b_i y_i}{\sum_{i=1}^{n} b_i^2} \tag{4}$$

Here, $\hat{\beta}_1$ and $\hat{\gamma}_1$ are the estimated regression coefficients for gestational age and BMI, respectively.

2.2. Results and Analysis

Table 1displays the correlation coefficient matrix among gestational age, BMI, and the mean-centered Y chromosome concentration values. It can be observed that the correlation coefficient between gestational age and Y chromosome concentration is 0.492, and that between BMI and Y chromosome concentration is 0.397. This indicates a moderate positive correlation between both variables and Y chromosome concentration.

Table 1. Correlation Coefficient Matrix.

	Gestational Age	BMI Maternal BMI	Y Chromosome Concentration
Gestational Age	1.000	0.590073	0.491912
Maternal BMI	0.590073	1.000	0.396787
Y Chromosome Concentration	0.491912	0.396787	1.000

To more intuitively visualize the association patterns and distribution characteristics between the variables, scatter plots with regression lines were generated for gestational age versus Y chromosome concentration and BMI versus Y chromosome concentration, as shown in Figure 2. The scatter distribution clearly shows that as both gestational age and BMI increase, the Y chromosome concentration exhibits a noticeable upward trend. Furthermore, the data points are closely distributed along the regression lines, further confirming the linear positive association between these two variables and Y chromosome concentration.

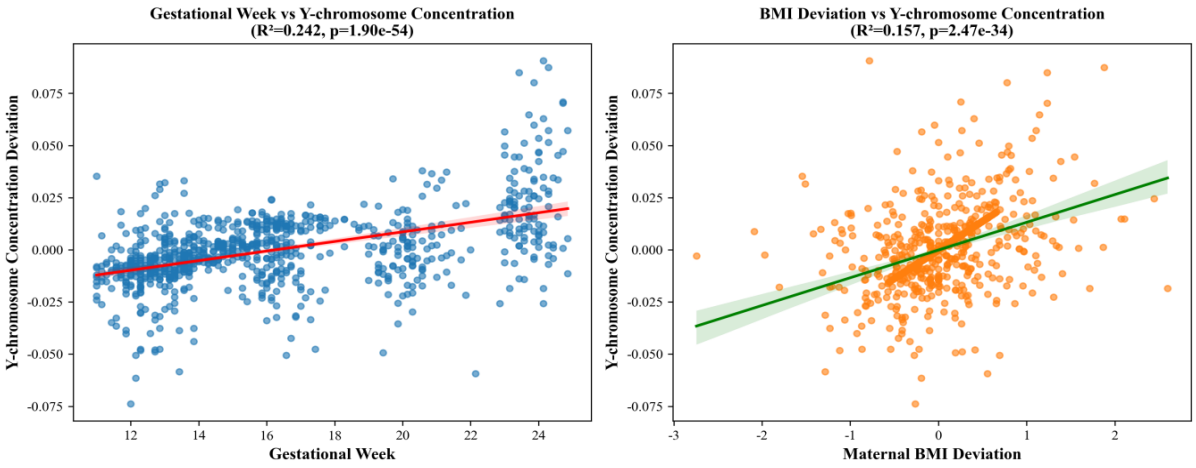

Figure 2. Regression Plots of Fetal Y Chromosome Concentration against Gestational Age and BMI.

The significance test results (p-values) for the correlations between the variables, based on the regression results, are presented in Table 2. All p-values are substantially lower than the significance level of 0.05, indicating that the observed correlations are statistically significant. The p-value for the correlation between gestational age and Y chromosome concentration is 1.90×10^{-54}, and the p-value for the correlation between BMI and Y chromosome concentration is 2.47×10^{-34}. Both are highly significant, providing substantial statistical evidence for establishing regression models.

Table 2. Matrix of Significance P-values.

Metric	Gestational Age	Maternal BMI	Y Chromosome Concentration
Gestational Age	0.000000e+00	4.145542e-83	1.903862e-54
Maternal BMI	4.145542e-83	0.000000e+00	2.468204e-34
Y Chromosome Concentration	1.903862e-54	2.468204e-34	0.000000e+00

3. Study on BMI Stratification and Optimal NIPT Testing Time for Male Pregnancies

3.1. Methodology for BMI Stratification and Optimal NIPT Testing Time Research

3.1.1. Definition of Event Time and Censoring Variables

The reliability of NIPT depends on the concentration of cell-free fetal DNA (FF), with a 4% threshold commonly used in clinical practice as the minimum reliable standard. This study models the "gestational week when the Y-chromosome concentration first reaches 4%" as the event time and utilizes survival analysis methods to estimate the earliest testing time for different BMI groups. Let $Y_i(w)$ denote the Y-chromosome concentration for the i-th pregnant woman at gestational week w. Her event time is then defined as:

$$T_i = \inf\{w : Y_i(w) \geq 0.04\} \tag{5}$$

If the threshold is not met during the follow-up period, it is considered right-censored; if it is only known that the threshold was met between two time points, it is considered interval-censored. A censoring indicator variable is constructed:

$$X_i = \min(T_i, C_i), \quad \delta_i = \begin{cases} 1, & T_i \leq C_i \\ 0, & T_i > C_i \end{cases} \tag{6}$$

Where C_i represents the censoring gestational week (end of follow-up) for this individual, and δ_i is the event indicator variable.

3.1.2. BMI Stratification Based on K-means Clustering

Since BMI is a significant factor influencing the concentration of cell-free fetal DNA, K-means clustering was employed to automatically partition pregnant women into BMI intervals, thereby avoiding subjective grouping bias. Its objective function is:

$$\min_{\{\mu_g\},\{c_i\}} \sum_{g=1}^{K} \sum_{i:c_i=g} |x_i - \mu_g|^2 \tag{7}$$

Where x_i is the BMI of the pregnant woman, μ_g is the center of the g-th cluster, and c_i indicates the cluster assignment. The optimal number of clusters K was determined jointly using the Elbow Method and the Silhouette Score Method, ultimately dividing maternal BMI into distinct intervals.

3.1.3. Kaplan-Meier Survival Function Estimation

For each BMI group g, the survival function is defined as:

$$S_g(w) = \Pr(T > w \mid grp = g) \tag{8}$$

The event time was non-parametrically estimated using the Kaplan-Meier method,

$$\hat{S}_g(w) = \prod_{t_{j,g} \le w} \left(1 - \frac{d_{j,g}}{n_{j,g}}\right) \tag{9}$$

Where $t_{j,g}$ is the gestational week at which the j-th event occurs, $d_{j,g}$ is the number of events at that week, and $n_{j,g}$ is the number of individuals at risk.

$$\hat{F}_g(w) = 1 - \hat{S}_g(w) \tag{10}$$

3.2. Results and Analysis

3.2.1. BMI Clustering Results

The rationality of the cluster number was verified using the Elbow Method and the Silhouette Score Method, with the results shown in Figure 3. The left plot shows a distinct inflection point in clustering inertia when k=3, indicating a significant reduction in within-group variance at this point. The right plot shows that the silhouette score peaks when k=3, indicating the highest within-cluster similarity and the most significant between-cluster separation for this number of clusters. Comprehensively, the optimal number of clusters was determined to be 3.

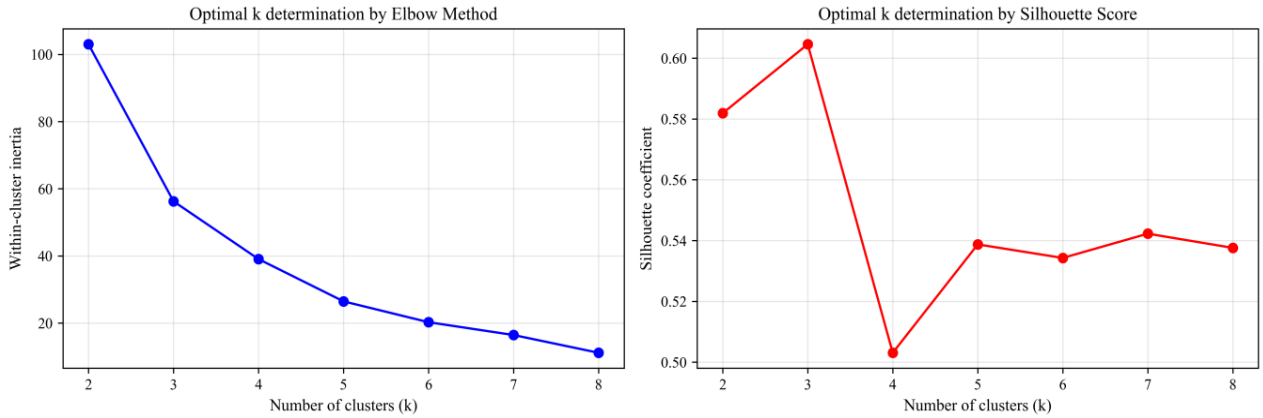

Figure 3. Determination of the Optimal Number of Clusters by Elbow Method and Silhouette Coefficient.

The final grouping results are shown in Table 3.

Table 3. BMI Grouping Results.

BMI Group	BMI Lower Limit	BMI Upper Limit	BMI Mean
Group 1	20.70	32.23	30.23
Group 2	32.36	37.55	34.29
Group 3	38.76	46.88	41.35

3.2.2. Optimal NIPT Testing Time for Different BMI Groups

The survival curves plotted based on the estimation results are shown in Figure 4. The figure shows that the low-BMI group typically meets the 80% threshold attainment condition around weeks 10-11, the medium-BMI group around weeks 11-12, while the high-BMI group requires until weeks 12-13 to ensure 90% threshold attainment. The differences between the groups are substantial.

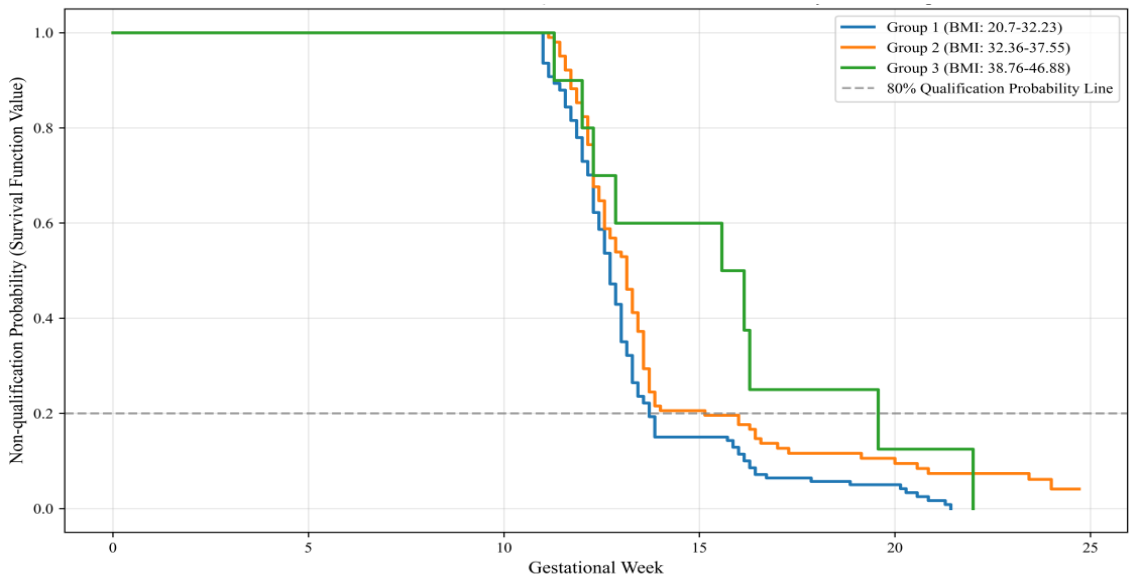

Figure 4. Survival Curves of Y-chromosome Concentration Reaching the Threshold for Different BMI Groups.

Based on the estimation results from the actual data, the optimal testing times for different BMI groups show significant differences, as presented in Table 4.

Table 4. Optimal NIPT Testing Time for Each Group.

BMI Group	BMI Range	Optimal NIPT Timepoint	Sample Size
Group 1	20.70–32.23	13.71	141
Group 2	32.36–37.55	15.14	102
Group 3	38.76–46.88	19.57	10

As can be seen from the table, the optimal testing timepoints for pregnant women in different BMI groups differ significantly. Further Log-rank test results showed that the differences in survival curves among the different BMI groups were statistically significant ($p < 0.05$), indicating that the influence of BMI on the optimal NIPT testing gestational week cannot be ignored.

3.2.3. Impact of Detection Error on the Optimal Testing Time

The results based on Monte Carlo simulation (100 iterations) are shown in Table 5.The standard deviation of the optimal timepoint was 0.23 weeks for the low-BMI group, indicating minimal influence from error; it was 0.91 weeks for the medium-BMI group, indicating moderate fluctuation; and 1.72 weeks for the high-BMI group, indicating that this group is significantly affected by error interference.

Table 5. Analysis of the Impact of Detection Error (100 Simulations).

BMI Group	Mean Optimal Timepoint	Std Dev of Optimal Timepoint	Maximum
Group 1	13.83	0.23	1.71
Group 2	14.99	0.91	2.71
Group 3	20.19	1.72	7.00

To visually demonstrate the differences in error impact, a box plot of the optimal timepoint distribution was drawn, as shown in Figure 5.

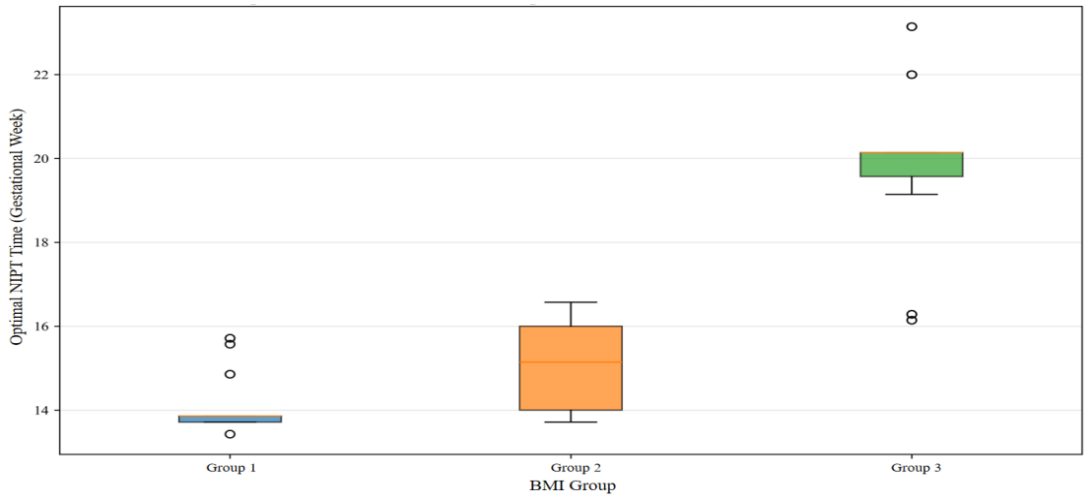

Figure 5. Impact of Testing Error on Optimal NIPT Timing (Monte Carlo Simulation).

The box plot results clearly illustrate the error tolerance of the different BMI groups. The low-BMI group shows the smallest data dispersion, where error interference is negligible; the high-BMI group shows the largest dispersion, where error can lead to a substantial delay in the timepoint. This suggests that testing for high-BMI pregnant women should be appropriately delayed from the original optimal timepoint to counteract the risk of failure introduced by error.

4. Optimization of the Optimal NIPT Testing Time under Multi-Factor Stratification

4.1. Methodology for Rational BMI Grouping and Optimal NIPT Testing Time Optimization

4.1.1. Population Stratification

On the basis of the previous analysis, multiple factors are further integrated. By introducing stratification optimization based on age and parity, the samples are divided into four independent populations: the parous group, the nulliparous group, the ≤30 years old group, and the >30 years old group.

4.1.2. BMI Subgroup Division and Event Time Definition

Within each major group, further subdivision was performed based on maternal BMI. The K-means clustering method was used to automatically determine the number of subgroups k, optimized using the silhouette coefficient:

$$s(k) = \frac{1}{n}\sum_{i=1}^{n}\frac{b(i) - a(i)}{\max\{a(i), b(i)\}} \tag{11}$$

Where a(i) is the average distance between sample i and other points in the same cluster, and b(i) is the average distance between sample i and points in the nearest neighboring cluster. The value of k corresponding to the maximum s(k) was selected as the optimal number of subgroups.

The definitions of event time and censoring variable followed the previous logic. For each pregnant woman, an event was considered to have occurred if Y≥0.04 was detected for the first time at gestational week t. Otherwise, it was considered censored:

$$T_i = \min\{t \mid Y_i(t) \geq 0.04\}$$
$$\delta_i = \begin{cases} 1, & \text{if there exists a } t \text{ such that } Y_i(t) \geq 0.04, \\ 0, & \text{otherwise } (censored). \end{cases} \tag{12}$$

Where T_i is the event time and δ_i is the event indicator variable.

4.1.3. Baseline Timepoint Estimation and Detection Error Simulation

Within each BMI subgroup, the Kaplan-Meier method was used to estimate the "probability of not meeting the threshold" curve. To evaluate the impact of detection error on the timepoint estimation, a normal disturbance simulation was constructed based on the standard deviation of the actual sequencing data $\sigma = 0.007967$, adding random noise to the Y-chromosome concentration:

$$Y_{\text{sim}} = \max(Y + \varepsilon, 0), \quad \varepsilon \sim \mathcal{N}(0, \sigma^2) \tag{13}$$

The simulation was repeated 100 times, the distribution of optimal timepoints $\{t_1^*, t_2^*, \text{dots}, t_{100}^*\}$ from each run was recorded, and the following were calculated:

$$\mu_t = \frac{1}{100}\sum_{i=1}^{100} t_i^*, \quad \sigma_t = \sqrt{\frac{1}{100}\sum_{i=1}^{100}(t_i^* - \mu_t)^2} \tag{14}$$

4.1.4. Timepoint Optimization Based on Detection Success Rate

A candidate timepoint interval was set around the baseline timepoint t^*:

$$\mathcal{T} = \{t^* - 2, t^* - 1.8, ..., t^* + 2\} \tag{15}$$

For each candidate timepoint $t \in \mathcal{T}$, the detection success rate was calculated:

$$R(t) = \frac{1}{N}\sum_{i=1}^{N} I\left(\frac{Q_i}{M_i} \geq 0.04 \bigwedge T_i \leq t\right) \tag{16}$$

Where N is the total number of pregnant women in the subgroup, Q_i is the number of successful tests (meeting threshold) for the i-th woman, M_i is her total number of tests, and $I(\cdot)$ is the indicator function. The gestational week with the highest success rate was ultimately selected as the optimized timepoint.

4.2. Results and Analysis

4.2.1. Optimized Optimal NIPT Testing Timepoints for Each Stratum

Based on Kaplan-Meier survival analysis and success rate optimization, the optimal testing timepoints and optimization effects for different BMI subgroups within each stratum are shown in Tables 6 and 7.

Table 6. Optimal NIPT Timepoints and Optimization Results for Parous and Nulliparous Groups.

	Group	BMI Subgroup	BMI Range	Optimal Timepoint	Number of Wo	Group
Parous	BMI1	27.7–33.8	13.86	58	15.26	84.48
	BMI2	34.4–45.0	19.57	19	19.77	84.21
Nulliparous	BMI1	20.7–32.5	13.71	104	13.91	84.62
	BMI2	32.6–46.9	16.00	72	17.40	87.50

Table 7. Optimal NIPT Timepoints and Optimization Results for Age ≤30 and Age >30 Groups

	Group	BMI Subgroup	BMI Range	Optimal Timepoint	Number of Wo	Group
Age ≤30	BMI1	36.1–46.9	20.57	16	20.77	81.25
	BMI2	27.1–31.8	13.71	99	13.91	84.85
	BMI3	32.0–35.8	13.71	69	15.31	88.41
Age>30	BMI1	28.1–32.4	13.86	36	14.06	80.56
	BMI2	38.8–45.0	22.00	4	22.20	100.00
	BMI3	32.7–37.1	16.00	28	16.60	89.29
	BMI4	20.7–20.7	16.29	1	16.49	100.00

In the grouping results, the optimal testing time for parous women with low BMI was significantly earlier than for those with high BMI. For women with BMI 27.7—33.8, the timepoint was delayed from 13.86 weeks to 15.26 weeks, increasing the success rate to 84.48%.Nulliparous women with high BMI required a delay until approximately 17.40 weeks, achieving a success rate of 87.50%.In the age stratification, high-BMI women in the >30 age group required a delay until approximately 22 weeks to ensure a success rate close to 100%, while the differences within the ≤30 age group were relatively smaller. Overall, the higher the BMI, the later the optimal testing timepoint. This indicates that advanced maternal age makes women more susceptible to the influence of BMI, and particularly those with high BMI require later testing to ensure success rates.

4.2.2. Comparison of Optimized Success Rates Across Strata

To compare the differences in optimized NIPT testing outcomes across different groups, a comparison chart of success rates for each BMI subgroup was plotted, as shown in Figure 6.

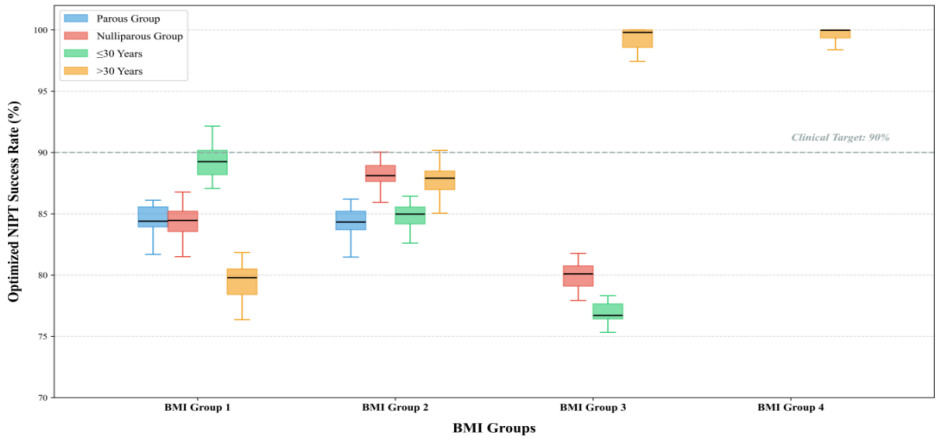

Figure 6. Comparison of Optimized NIPT Success Rates of BMI Subgroups in the Four Groups.

From the figure, it can be observed that the success rates for some BMI subgroups in the >30 age group are close to or reach 100%, significantly exceeding the clinical target of 90%. In contrast, the success rates for the parous and nulliparous groups are generally slightly lower, mostly remaining around 84%—88%.This result indicates that for women of advanced maternal age, appropriately delaying testing can significantly increase the success rate; whereas for younger or primiparous women, more refined timepoint optimization strategies are needed to narrow the gap with the clinical target.

To compare the changes in the optimal NIPT testing timepoints before and after optimization across different groups, a comparison chart of gestational weeks for each BMI subgroup was plotted, as shown in Figure 7.

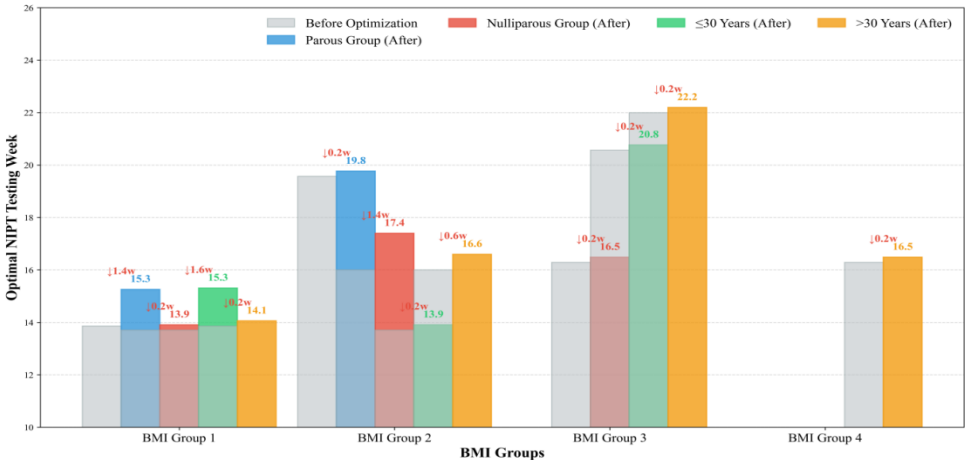

Figure 7. Comparison of Differences in NIPT Testing Timing Before and After Optimization in the Four Groups.

The results show that after optimization, the testing timepoints for most BMI subgroups were delayed by approximately 0.2 weeks overall, indicating a small magnitude of change. However, the optimal testing timepoint for the high-BMI population remains significantly later than that for the low-BMI population. Clinically, this suggests that for high-BMI pregnant women, moderately delaying testing helps improve the success rate, but testing too late may shorten the intervention window for abnormal fetuses. Therefore, in practical applications, a balance must be struck between "increasing success rate" and "early risk detection".

5. Conclusion and Implications

Under the widespread application of non-invasive prenatal testing (NIPT), imprecise test timing and significant individual variability have emerged as key factors affecting test success rates and clinical decision-making. This study proposes a personalized testing time optimization model based on individual characteristics, which holds substantial value for enhancing NIPT effectiveness and accuracy. By analyzing fetal cell-free DNA (cfDNA) concentrations relative to gestational age and maternal BMI, we identified moderate positive correlations between both gestational age and BMI with Y-chromosome concentration (as a proxy for fetal fraction). K-means clustering combined with Kaplan-Meier analysis revealed detectable fetal fractions at approximately 13.71 weeks for low-BMI groups and after 19.57 weeks for high-BMI groups. Monte Carlo simulations demonstrated that high-BMI populations experience greater signal fluctuations, suggesting delayed testing is preferable. When stratifying by age and obstetric history, higher BMI correlated with later optimal testing windows, reaching nearly 22 weeks for high-BMI women over 30. By balancing early detection with high success probability through candidate window scanning, our optimized strategy achieved an overall success rate exceeding 84% and 100% in high-risk subgroups, validating its effectiveness. These findings highlight that individual characteristics significantly influence NIPT outcomes, rendering universal fixed testing windows inadequate. A stratified model integrating BMI clustering, survival analysis, and multivariate stratification can provide tailored testing recommendations for diverse populations.

For the future development and practical implementation of NIPT, we propose the following recommendations:

1. Clinical Practice Recommendations: NIPT performance depends on maternal physiological traits. Healthcare providers should systematically collect BMI, age, and reproductive history before testing to determine personalized schedules using the proposed model, minimizing premature testing failures and repeat procedures. Concurrently, clinician training on technical limitations should be prioritized to manage patient expectations and reduce anxiety related to potential misinterpretations.

2. Technological Development Recommendations: While promising, the current model is constrained by sample size and data availability. Future research should prioritize multi-center collaborations with large, diverse cohorts to validate generalizability. Integrating advanced machine learning, particularly deep learning frameworks, could enhance high-dimensional data processing and identify novel biomarkers to improve model performance.

3. Health Education Recommendations: Pregnant individuals require clear health literacy to engage effectively with screening protocols. Healthcare institutions should standardize patient education on NIPT principles, clinical scope, and limitations, emphasizing the rationale for delayed testing or supplementary diagnostics in high-BMI and advanced-age populations. Tailored screening pathways for these groups can ensure reliable risk assessment while maintaining diagnostic confidence.

References

[1] Norton, M. E., Jacobsson, B., & Edmonds, J. K. Noninvasive prenatal testing: current and future applications in clinical practice[J]. Obstetrics and Gynecology, 2023, 141(4): 767-781

[2] Gil, M. M., Quezada, M. S., Revello, R., Akolekar, R., & Nicolaides, K. H. Maternal body mass index and cell-free DNA screening test failure: a systematic review and meta-analysis[J]. Ultrasound in Obstetrics & Gynecology, 2021, 57(4): 553-563.

[3] Benn, P., & Chapman, M. Non-invasive prenatal testing for trisomy 21: the importance of adjusting for maternal age and gestational age[J]. Prenatal Diagnosis, 2022, 42(8): 983-990.

[4] Jiaxin Li, Yuan Wei, Yangyu Zhao. Progress in non-invasive prenatal testing failure due to less cell-free fetal DNA [J]. Chinese Journal of Perinatal Medicine,2019,22(1):30-34.

[5] Pengyu Chen, Quanfu Zhang. Advances in the Influencing Factors and Clinical Application of Fetal Fraction of the Non-Invasive Prenatal Testing [J]. Advances in Clinical Medicine,2024(10):1183.

[6] Gazdarica J, Forgacova N, Sladecek T, et al. Insights into non-informative results from non-invasive prenatal screening through gestational age, maternal BMI, and age analyses[J]. PLOS ONE,2024, 19(3): e0280858.

[7] Duboc N, Smith M,Jones R, et al. NiPTUNE: A Bioinformatics Pipeline for Non-Invasive Prenatal Testing of Fetal Aneuploidy[J]. Briefings in Bioinformatics,2024,23(1): bbab380.

[8] Benn P, Borrell A, Chiu R W K, et al. Timing of cell-free DNA screening for aneuploidy: when is the optimal window? [J]. American Journal of Obstetrics and Gynecology, 2021, 224(1): 33-43.

[9] Srinivasan A, Bianchi D W, Huang H, et al. Serial measurements of fetal fraction in cell-free DNA from maternal plasma: implications for non-invasive prenatal testing[J]. Prenatal Diagnosis, 2021, 41(4): 467-474.

[10] van Beek E,de Vries M, Oepkes D, et al. Quality Control of Fetal Fraction Measurement in Non-Invasive Prenatal Testing[J]. Prenatal Diagnosis,2017,37(10):987-994.